Prediction of Magnetic Properties in Oxovanadium(IV) Phosphates: The Role of the Bridging PO_4 Anions

Manuel Roca,[†] Pedro Amorós,*[,†] Juan Cano,[‡] M. Dolores Marcos,[†] Jaime Alamo,[†] Aurelio Beltrán-Porter,[†] and Daniel Beltrán-Porter[†]

Institut de Ciència dels Materials de la Universitat de València (ICMUV) and the Departament de Química Inorgánica de la Universitat de València, Dr. Moliner No. 50, 46100 Burjassot (València), Spain

Received September 19, 1997

Oxovanadium phosphates constitute a crystallochemically very rich family that, in turn, results in a seemingly intricate magnetochemistry including from isolated dimers to 3-D systems. This magnetic diversity is due, in part, to the possible participation of phosphate groups in the spin transfer between V^{IV} centers. This way, ^{31}P solid-state NMR becomes a key tool in determining the exchange paths involving phosphorus orbitals. The magnetic behavior of several layered oxovanadium phosphates $M(VOPO_4)_2 \cdot 4H_2O$ ($M = Na^+$, Ca^{2+}, Ba^{2+}, and Pb^{2+}) has been investigated. Like it occurs in the case of other previously studied lamellar derivatives, the best fit of the temperature-dependent magnetic susceptibility data is obtained for a 2-D model. This is consistent with chairlike $V(OPO)_2V$ exchange pathways (i.e., through di-μ-(O,O′)phosphate bridges). Both these results and those previously available for other oxovanadium phosphates can be nicely correlated with the structural data focusing the attention on the topological features concerning the environment of the phosphate bridging entities, a result that is consistently rationalized on the basis of extended Hückel calculations. The reliability of our approach is supported not only by its ability to interpret the diversity of experimental magnetic behavior but also by its predictive character concerning the approximate magnitude of the superexchange interactions in other related derivatives.

Introduction

Magnetochemists have devoted much work in recent years to rationally design ligand environments able to define superexchange pathways leading to specific magnetic properties.[1] In practice, the results have been rather satisfactory in molecular systems with simple $S = {}^1/_2$ paramagnetic centers,[2] but the understanding of magnetic interactions in related extended systems remains ambiguous. Thus, in a recent publication, Le Bideau et al.[3] have elegantly raised some of the problems hindering a systematic approach to the coupling between magnetic orbitals in self-assembled extended arrays. In fact, their work on layered vanadyl phosphonates illustrates aspects of the role of the chairlike $V(OPO)_2V$ links between paramagnetic d^1-$V^{IV}O_6$ vanadyl centers as effective exchange pathways, a result that should be consistent with previous observations on related systems.[4−6] In contrast, Canadell et al.[7] conclude that there is no real participation of diamagnetic phosphate groups in magnetic exchange between d^1-$Mo^{V}O_6$ centers in molybdenum phosphates.

Actually, the possibility that multiatom oxo bridge units composed of high-symmetry oxoanions may act as suitable agents for the transfer of magnetic exchange interactions was not considered until the work of Reiff et al.[8] In the case of $[PO_4]$ entities, and when dealing with oxovanadium(IV) hydrogenphosphates, we found direct evidence of the involvement of phosphate bridging anions in the spin transfer between vanadium centers with the help of variable temperature solid-state ^{31}P NMR technique.[9] This result was then corroborated in the work of Lezama et al.[10] with $MoOPO_4$. Molybdenyl phosphate has in common with oxovanadium(IV) hydrogenphosphates the only presence of μ-(O,O′)PO_4 and oxo bridges (from the M═O groups) between paramagnetic d^1 centers, which makes them different from many of the complex structures considered in ref 7.

* To whom correspondence should be addressed. E-mail: pedro.amoros@UV.es.

[†] Institut de Ciència dels Materials de la Universitat de València (ICMUV).

[‡] Departament de Química Inorgánica de la Universitat de València.

(1) (a) Kahn, O. *Molecular Magnetism*; VCH: Weinheim, 1993. (b) *Magnetic Molecular Materials*; Gatteschi, D., Kahn, O., Miller, J. S., Palacio, F., Eds.; Kluwer: Dordrecht, 1991. (c) Miller, J. S.; Epstein, A. J. In *Materials Chemistry: An Emerging Discipline*; Advanced Chemistry Series 245; American Chemical Society: Washington, DC, 1995; p 161.

(2) (a) Hatfield, W. E. In *magnetostructural Correlations in Exchange Coupled Systems*; Willet, R. D., Gatteschi, D., Kahn, O., Eds.; NATO ASI Series; Reidel: Dordrecht, 1985. (b) Plass, W. *Angew. Chem., Int. Ed. Engl.* **1996**, *35*, 627.

(3) Le Bideau, J.; Papoutsakis, D.; Jackson, J. E.; Nocera, D. G. *J. Am. Chem. Soc.* **1997**, *119*, 1313.

(4) (a) Bond, M. R.; Mokry, L. M.; Otieno, T.; Thompson, J.; Carrano, C. J. *Inorg. Chem.* **1995**, *34*, 1894. (b) Otieno, T.; Mokry, L. M.; Bond, M. R.; Carrano, C. J.; Dean, N. S. *Inorg. Chem.* **1996**, *35*, 850.

(5) Papoutsakis, D.; Jackson, J. E.; Nocera, D. G. *Inorg. Chem.* **1996**, *35*, 800.

(6) Beltrán, D.; Beltrán, A.; Amorós, P.; Ibáñez, R.; Martínez, E.; Le Bail, A.; Ferey, G.; Villeneuve, G. *Eur. J. Solid State Inorg. Chem.* **1991**, *28*, 131.

(7) Canadell, E.; Provost, J.; Guesdon, A.; Borel, M. M.; Leclaire, A. *Chem. Mater.* **1997**, *9*, 68.

(8) Torardi, C. C.; Calabrese, J. C.; Lázár, K.; Reiff, W. M. *J. Solid State Chem.* **1984**, *51*, 376 and references therein.

(9) Villeneuve, G.; Suh, K. S.; Amorós, P.; Casañ-Pastor, N.; Beltrán, D. *Chem. Mater.* **1992**, *4*, 108.

(10) Lezama, L.; Villeneuve, G.; Rojo, T. *Solid State Commun.* **1990**, *76*, 449.

(11) Centi, G.; Trifiro, F.; Ebner, J. R.; Franchetti, V. M. *Chem. Rev.* **1988**, *88*, 55.

S0020-1669(97)01210-X CCC: $15.00
Published on Web 06/10/1998

Among the many reasons for studying the vanadium phosphate systems,[11,12] one of them is their possible usefulness in testing models of predictions of magnetic properties.[13] From the above, it appears that [PO_4] bridging entities can be involved in the magnetic exchange. To elucidate their role, it seems reasonable to study systematically the magnetic behavior of compounds in which there are no additional bridges (other than the inactive oxo vanadyl group), which excludes a great number of known structures.[14] Hence, we will focus our attention basically on two sets of vanadium phosphate systems, namely, oxovanadium(IV) hydrogenphosphates and $M(VOPO_4)_2{\cdot}nH_2O$ layered vanadyl phosphates. In fact, some partial results and hypotheses concerning mainly oxovanadium(IV) hydrogenphosphates were advanced in a previous publication,[13] and these ideas were successfully extended to related systems by other authors.[4,5] Notwithstanding, the attention we paid to approach a consistent topological magnetostructural correlation was then focused only on the relative position of the VO_6 octahedra, which together with the PO_4 tetrahedra define the structural framework. New magnetic data on layered oxovanadium(IV) phosphates and some indirect evidence[7] prompted us to reconsider all of the results from a new point of view: if the phosphate bridging anions play a relevant role in the spin transfer between vanadium centers, then the effectiveness of the exchange pathway should depend not only on the VO_6 octahedron arrangement but also the relative orientation of the PO_4 bridges.

We present here new magnetic results from layered oxovanadium(IV) phosphates, and both these and the previously available results are integrated in a topological scheme leading to a nice magnetostructural correlation that allows us to make reasonable predictions on the magnitude of the magnetic interaction in related solids. Detailed extended Hückel calculations clearly support the idea about the dependence of the exchange coupling with selected topological parameters in these series of phosphates.

Experimental Section

Synthesis. Experimental details concerning the synthesis of oxovanadium(IV) hydrogenphosphate hydrates are included elsewhere.[6,15] In short, these $VO(HPO_4){\cdot}nH_2O$ ($n = 0.5$, 2(α), 2(β), and 4) solids are prepared from V_2O_5 and H_3PO_4 using acetone/water media and iodhydric acid both as reducing agent and proton donor. The acetone/water ratio is the main variable determining the hydration degree of the final materials. In the absence of acetone, the resulting stable phase is $VO(H_2PO_4)_2$. $(VO)_2P_2O_7$ can be obtained by pyrolysis of the oxovanadium(IV) hydrogenphosphate hydrates under N_2 flowing atmosphere.[6,12]

The lamellar oxovanadium phosphates containing guest cations among layers, $M(VOPO_4)_2{\cdot}nH_2O$, have been prepared under soft hydrothermal conditions (200 °C, 2 days) according to the general procedure described in ref 16. The starting solutions contain V_2O_5/V/H_3PO_4/metal acetate/water in molar ratios 1/0.5/23/1/833 or 1/0.25/23/2/833, depending on the univalent or divalent character, respectively, of the guest cations. From the magnetic point of view, materials already characterized are those including Na, K, Rb, and Sr,[5] but results concerning the sodium derivative are contradictory.[17] To complete the information on this series of phosphates we have prepared, by using our general procedure,[16] the materials containing Na, Ca, Ba, and Pb as guest cations. Chemical analyses are as follows. Calcd (Found) for $Na(VOPO_4)_2{\cdot}4H_2O$: V, 24.33 (24.48); P, 14.79 (14.71); Na, 5.49 (5.40); water, 17.19 (17.30). Calcd (Found) for $Ca(VOPO_4)_2{\cdot}4H_2O$: V, 23.37 (23.42); P, 14.21 (14.10); Ca, 9.19 (9.25); water, 16.51 (16.55). Calcd (Found) for $Pb(VOPO_4)_2{\cdot}4H_2O$: V, 16.89 (17.00); P, 10.27 (10.15); Pb, 34.56 (34.55); water, 11.94 (11.89). Calcd (Found) for $Ba(VOPO_4)_2{\cdot}4H_2O$: V, 20.33 (20.50); P, 12.36 (12.40); Ba, 27.40 (27.85); water, 14.37 (14.25).

Methods and Instrumentation. Metal and phosphorus contents were determined, after dissolution of the solids in boiling concentrated nitric acid, by atomic absorption spectrometry (Perkin-Elmer Zeeman 5000). Water was determined thermogravimetrically with a TGA-7 Perkin-Elmer instrument under nitrogen atmosphere at a 5 °C/min heating rate.

X-ray powder diffraction patterns were recorded by means of a conventional angle-scanning Siemens D500 diffractometer using Cu Kα radiation in order to characterize the polycrystalline samples. Patterns were collected in steps of 0.04° (2θ) over the angular range 10−70° (2θ) for 8 s per step.

^{31}P NMR spectra were recorded at 80.962 MHz on a high-power Bruker MSL 200 spectrometer equipped with a 4.7 T superconducting magnet and using a solid echo sequence with phase cycling. The spectral width was 500 kHz. A magic angle spinning experiment was performed with the sodium-containing derivative. The line shifts were referenced to 85% H_3PO_4(aq) measured in the same probe. X-band ESR spectra were recorded on a Bruker ER 200D spectrometer.

Magnetic measurements were performed at 1000 G in the temperature range 2−300 K with a SQUID Quantum Design MPMS-XL-S susceptometer. Corrections for the diamagnetism of the compound were estimated using Pascal's constants.[18]

Results and Discussion

The entire set of oxovanadium(IV) phosphates whose magnetic behavior has been analyzed is listed in Table 1, which also includes the more significant results in the present context. Otherwise, the remarkable structural diversity of M/vanadium/phosphate (M = uni- or divalent cations) phases synthesized and characterized over the past few years has been considered from a variety of perspectives. To advance toward predicting magnetic properties in oxovanadium(IV) phosphates, we propose that attention be focused on the variation of the topological features of the structural fragments that define the paramagnetic pseudomolecular blocks whose spatial propagation would reproduce the currently determined crystal structures. The scaled pictures in Figure 1 correspond to the representative building blocks experimentally found in the structures of solids in Table 1. Both these blocks and data in Table 1 are the basis of the experimental and theoretical study that follows.

^{31}P Nuclear Magnetic Resonance Results. The involvement of phosphate groups in the spin density transfer between V^{IV} was established with the help of variable temperature solid-state ^{31}P NMR in the case of hydrogen phosphate derivatives.[6,9] The presence of finite spin density at the phosphorus nuclei was related with the shift of the ^{31}P NMR signals from the diamagnetic standard, and correlations between the NMR line shifts and the exchange constants allowed us to discuss the

(12) Amorós, P.; Ibáñez, R.; Beltrán, A.; Beltrán, D.; Fuertes, A.; Gómez-Romero, P.; Hernandez, E.; Rodriguez-Carvajal, J. *Chem. Mater.* **1991**, *3*, 407.
(13) (a) Amorós, P.; Beltrán, A.; Beltrán, D. *J. Alloys Compd.* **1992**, *188*, 123. (b) Villeneuve, G.; Amorós, P.; Drillon, M. In *Organic and Inorganic Low-Dimensional Crystalline Materials*; Delhaes, P., Drillon, M., Eds.; NATO ASI Series B168; Plenum: New York, 1987. (c) Beltrán, D.; Amorós, P.; Ibáñez, R.; Martínez, E.; Beltrán, A.; Le Bail, A.; Ferey, G.; Villeneuve, G. *Solid State Ionics* **1989**, *32*, 57.
(14) (a) Lee, Y.-S.; Zubieta, J.; Haushalter, R.; O'Connor, C. J. *Mol. Cryst. Liq. Cryst.* **1995**, *274*, 79. (b) Zubieta, J. *Comments in Inorg. Chem.* **1994**, *16*, 153.
(15) Amorós, P.; Ibáñez, R.; Martínez, R.; Beltrán, A.; Beltrán, D.; Villeneuve, G. *Mater. Res. Bull.* **1989**, *24*, 1347.
(16) Roca, M.; Marcos, M. D.; Amorós, P.; Alamo, J.; Beltrán, A.; Beltrán, D. *Inorg. Chem.* **1997**, *36*, 3414.
(17) Sisková, R.; Benes, L.; Zima, V.; Vlcek, M.; Votinsky, J.; Kalousová, J. *Polyhedron* **1993**, *12*, 181.
(18) Boudreaux, E. A.; Mulay, L. N. *Theory and Applications of Molecular Paramagnetism*; John Wiley & Sons: New York, 1976; p 491.
(19) Harrison, W. T. A.; Lim, S. C.; Vaughey, J. T.; Jacobson, A. J.; Goshorn, D. P.; Johnson, J. W. *J. Solid State Chem.* **1994**, *113*, 444.

Table 1. Selected Magnetic Data for different Oxovanadium Phosphates

solid	C[a]	θ (K)	$T_{\chi_{max}}$ (K)	μ_{eff}[b] (μ_B)	model[c]	J (K)	δ (ppm)	ref
$(VO)_2P_2O_7$	0.772	−84.1	79.6	1.75	HAMC	−65.7	2000	6
					($\alpha = 0.7$)		2500	
$VO(HPO_4)\cdot 0.5H_2O$	0.371	−25.0	55.0	1.72	HD	−43.0	1736	6
α-$VO(HPO_4)\cdot 2H_2O$	0.365	−12.2	25.0	1.71	HD	−23.0	1360	9
β-$VO(HPO_4)\cdot 2H_2O$	0.370	−3.7	7.1	1.72	HLMC	−5.0	650	6
$VO(HPO_4)\cdot 4H_2O$	0.367	−4.5	6.0	1.71	HLMC	−4.7		6
$VO(H_2PO_4)_2$	0.358	−2.0	3.0	1.69	HLMC	−2.0	5	6
$Na(VOPO_4)_2\cdot 4H_2O$	0.369	−7.1	2.7	1.72	2-D	−2.3	100	this work
$Ca(VOPO_4)_2\cdot 4H_2O$	0.741	−7.7	4.1	1.72	2-D	−2.9	190	this work
$Pb(VOPO_4)_2\cdot 4H_2O$	0.760	−7.9	5.0	1.74	2-D	−2.8		this work
$Sr(VOPO_4)_2\cdot 4H_2O$					2-D	−2.5		5
$Ba(VOPO_4)_2\cdot 4H_2O$	0.742	−5.8	3.8	1.72	2-D	−2.1		this work
$Ba_2VO(PO_4)_2\cdot H_2O$	0.461	−8.5	10.0	1.92		−8−10[d]		19

[a] Units in emu·K·mol^{-1}. [b] Magnetic moment (in Bohr magnetons) per vanadium atom. [c] Hamiltonians used to model the experimental magnetic data: HAMC, $H = -2J\sum_i(S_{2i}S_{2i+1} + \alpha S_{2i}S_{2i-1})$ (Heisenberg alternating magnetic chain); HD, $H = -2JS_iS_j$ (isotropic Heisenberg dimer); HLMC, $H = -2J\sum_i(S_iS_{i+1})$ (Heisenberg linear magnetic chain); 2-D, $H = -2J\sum_{i,j}(S_iS_j)$ (Heisenberg square planar lattice). [d] Approximate value.

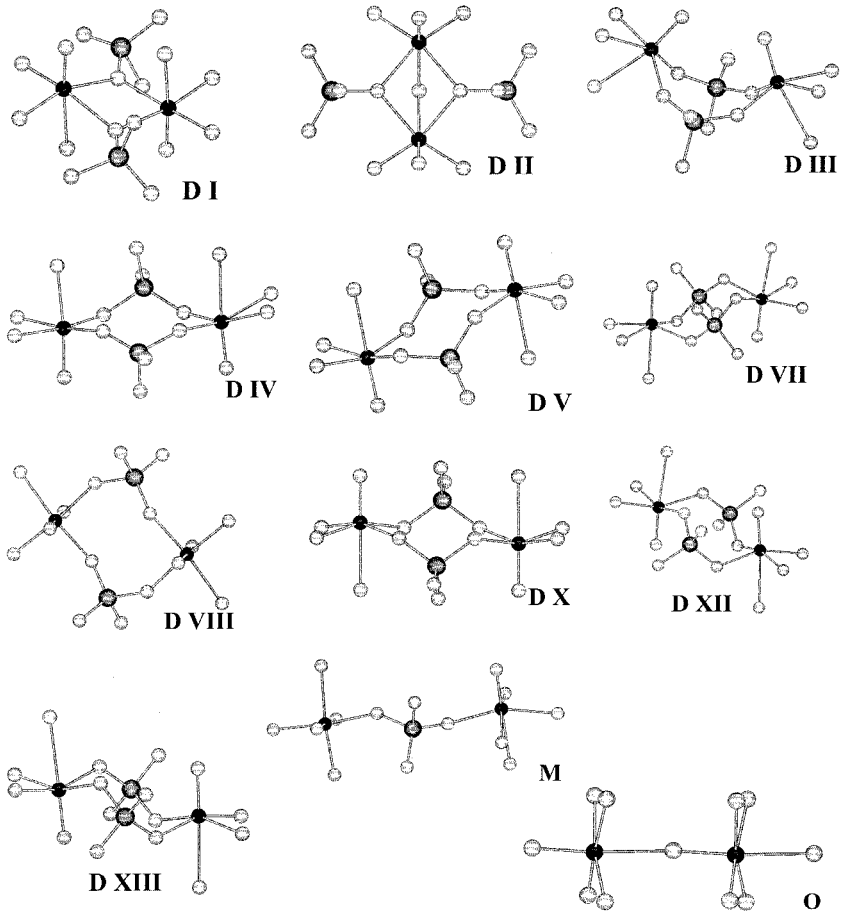

Figure 1. Representative building blocks observed in several known structures of oxovanadium phosphates. DI, DIV, and DVIII in $(VO)_2P_2O_7$. DII, DIII, and DVIII in $VO(HPO_4)\cdot 0.5H_2O$. DV in α-$VO(HPO_4)\cdot 2H_2O$. DVII in $VO(HPO_4)\cdot 4H_2O$. DX in $Ba_2VO(PO_4)_2\cdot H_2O$. DXII in $Ca(VOPO_4)_2\cdot 4H_2O$. DXIII in $Ba(VOPO_4)_2\cdot 4H_2O$. "D" corresponds to di-μ(O,O′)PO_4 (V(OPO)$_2$V chairlike type) or di-μ-(O)PO_4 bridges. M and O labels refer to the magnetically less effective μ-(O,O′)PO_4 and oxo (V═O) bridges, respectively.

contribution of the phosphate molecular orbitals to the magnetic orbitals. In terms of the molecular building blocks, there is no reason to expect alternative behaviors for the layered oxovanadium phosphates. In fact, the chairlike V(OPO$_2$)V links in $M(VOPO_4)_2\cdot nH_2O$ vary typically between those of the type DXII ($Ca(VOPO_4)_2\cdot 4H_2O$) and DXIII ($Ba(VOPO_4)_2\cdot 4H_2O$) (Figure 1), i.e. they are similar to those found in $VO(HPO_4)\cdot 4H_2O$ (DVII).[6,20] In practice, the results (Table 1) are as expected: in all cases the ^{31}P NMR signals appear slightly shifted from the standard, indicating weak magnetic exchange coupling. Moreover, as shown in Figure 2, both the δ values now determined for the $M(VOPO_4)_2\cdot nH_2O$ solids and those previously available for $VO(HPO_4)\cdot nH_2O$ (Table 1) fit well in the same J vs δ correlation curve. The fact that, considered as a whole, the J vs δ correlation be independent of the dimensionality of the magnetic interactions (see below) clearly supports the idea that it is the topological parameters of the phosphate bridges in the building blocks that determine the nature of the active magnetic exchange pathways (i.e., the

(20) Leonowicz, M. E.; Johnson, J. W.; Brodi, J. F.; Shanson, H. F.; Newsam, J. M. *J. Solid State Chem.* **1985**, *56*, 370.

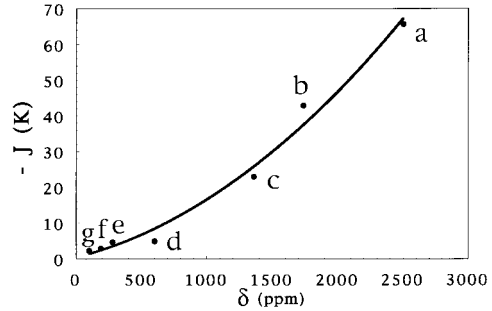

Figure 2. Observed correlation between the magnitude of the magnetic interaction measured as J and the experimental δ(ppm) from ^{31}P solid-state NMR experiments for different solids: (a) = $(VO)_2P_2O_7$, (b) = $VO(HPO_4)\cdot 0.5H_2O$, (c) = α-$VO(HPO_4)\cdot 2H_2O$, (d) = β-$VO(HPO_4)\cdot 2H_2O$, (e) = $VO(HPO_4)\cdot 4H_2O$, (f) = $Ca(VOPO_4)_2\cdot 4H_2O$, (g) = $Na(VOPO_4)_2\cdot 4H_2O$.

participation of phosphate molecular orbitals in the magnetic orbitals).

A particular case which deserves a comment because of the contradictory results in the literature is that concerning the V^{IV}/V^{V} mixed valence intercalates, i.e. $M(VOPO_4)_2\cdot nH_2O$ solids with M = univalent cations (Na^+, K^+, Rb^+). Thus, in contrast to earlier magnetic measurements,[17] Papoutsakis et al.[5] pointed to potential problems due to the synthesis method and concluded that ferromagnetic coupling occurs in the layers in these intercalates, which correlates with the parallel arrangement of the basal planes of [VO_6] octahedra throughout the entire framework. A question postponed for further study was referred to the possibility of itinerant magnetic behavior by electron hopping from V^{IV} to neighboring V^{V} sites. Actually, as shown below, both our experimental results and theoretical calculations indicate that coupling in the intercalates is antiferromagnetic. That is to say, our magnetic results should be consistent with Siskova's data,[17] despite the synthesis method used that, as mentioned in the work of Papoutsakis et al.,[5] includes hydrothermal treatment and not reduction by iodide.[21] In this context a ^{31}P NMR magic angle spinning experiment can throw some light on this subject. Thus, shown in Figure 3 is the spectrum corresponding to the sodium derivative. Three clearly distinguishable shifted main signals appear, showing an integrated area relationship of ca. 1:2:1, and a significantly minor unshifted signal. Then, there is no doubt on the presence of finite spin density at the P nuclei. Moreover, the proper presence of three different signals eliminates any possibility of two symmetrically related V^{IV}/V^{V} sublattices (what would result in a unique ^{31}P NMR shifted signal) and clearly points toward a random distribution of the paramagnetic centers. In this sense, it would show the existence of a statistically predominant type of phosphorus nuclei (δ = 89.7 ppm), which would see two V^{IV} centers (it is also well to remember that there exists an equimolar V^{IV}/V^{V} distribution in the lattice), and two other associated to the signals of half-intensity (δ = 66.8, 143.0 ppm) that might be understood as the ^{31}P seeing one or three V^{IV} paramagnetic centers. All this makes it reasonable to consider the localization of the unpaired electron, as indicated by the Siskova's conclusions based on the nonconducting character of $[VOPO_4]_\infty$ layers.[17] The possibility of itinerant magnetic behavior seems thereby a hazardous hypothesis.

(21) Papoutsakis et al.[5] indicate that their experience show that the iodide synthesis method can lead to samples with variable magnetic behavior (i.e., to different products). In our case, it must be stressed that the X-ray powder diffraction patterns of the samples whose magnetic behavior we are studying are coincident with those calculated from the single-crystal data reported in ref 22 for $M(VOPO_4)\cdot nH_2O$ (M = Ca, Sr, Pb) and ref 23 for M = Na, K.

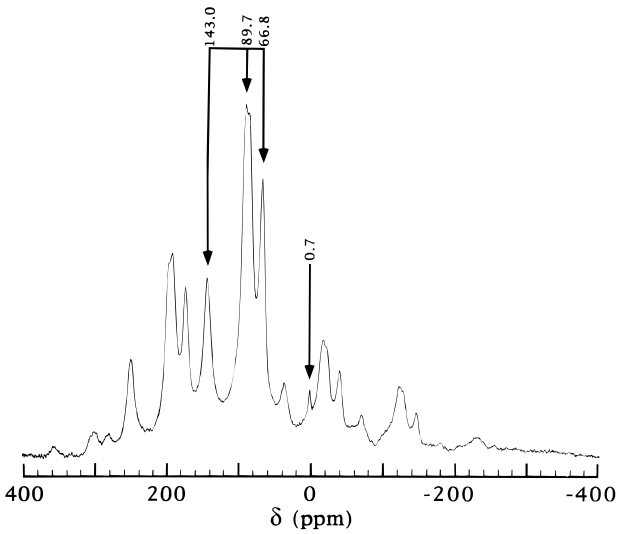

Figure 3. Magic angle spinning ^{31}P NMR spectra of $Na(VOPO_4)_2\cdot 4H_2O$ showing three slightly shifted signals.

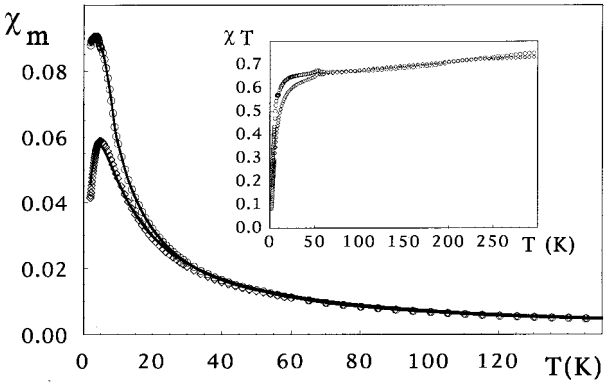

Figure 4. Thermal dependence of the molar magnetic susceptibility for $Pb(VOPO_4)_2\cdot 4H_2O$ (□) and $Ba(VOPO_4)_2\cdot 4H_2O$ (○). In the inset, their $\chi_m T$ vs T plots are represented.

Magnetic Properties. Susceptibility data for $M(VOPO_4)_2\cdot nH_2O$ (M = Na, Ca, Ba, Pb) show the onset of magnetic ordering at ~4−5 K and Curie−Weiss type paramagnetic behavior over the high-temperature range. The paramagnetic data are well described by using a Curie−Weiss type law: $\chi = C/(T - \theta)$, where χ is the measured magnetic susceptibility, C the Curie constant, T the temperature (K), and θ the Weiss constant. The best fit values are summarized in Table 1. The C values are consistent with the number of unpaired electrons per formula, indicating good agreement between the chemical analysis and magnetic data. In all cases, the negative values of θ indicate that the prevailing interactions are antiferromagnetic. At low temperatures the magnetic susceptibility of the samples shows a broad maximum, characteristic of magnetic exchange coupling between vanadium(IV) centers. Figure 4 shows the temperature-dependent magnetic susceptibilities for the lead and barium containing lamellar derivatives. The thermal variation of the χT product (inset of Figure 4), which exhibits a strong decrease below 20 K clearly confirms the antiferromagnetic nature of the interactions. We have chosen these cases because they represent the two extreme ones in this series in that concerning the relative arrangement of the medium basal planes of the VO_6 octahedra: parallel in the case of the Ba derivative[16] and defining the relatively highest dihedral angle (2.8°) in the case of the Pb compound.[22] As suggested above, the experimental behavior of calcium (2.6°)[22] and sodium

(~0°)[23] derivatives responds to a similar antiferromagnetic pattern.

Both from the structural and the magnetic points of view, the dominant building blocks in these solids are the chairlike $V(OPO)_2V$ units that expand along the *a* and *b* directions, leading to the characteristic layers.[16,22,23] Hence, given that we are treating lamellar solids and considering the spin density on the V^{IV} atoms in the layers to be located in the d_{xy} orbitals, it seems reasonable to neglect the importance of magnetic interactions between adjacent layers. Thus, magnetic susceptibility could be expressed, according to Rushbrooke and Wood (for $kT > J$),[24] as a high-temperature expansion series for a $S = {}^1/_2$ antiferromagnetic Heisenberg square planar lattice ($H = -2J\Sigma_{i,j} S_iS_j$):

$$\chi_m = \frac{Ng^2\beta^2}{4kT}\left[1 + \frac{2}{x} + \frac{2}{x^2} + \frac{1.333}{x^3} + \frac{0.250}{x^4} - \frac{0.4833}{x^5} + \frac{0.0013}{x^6}\right]^{-1}$$

with $x = kT/|J|$. The *J/k* values of Table 1 were obtained from fits of this last equation. Solid lines in Figure 4 represent the best fits obtained for calcium and barium derivatives.

It is true that our results differ in this way from those reported by Papoutsakis et al.,[5] but, in any case, it should be taken into account that we are dealing with weak resulting interactions. That is to say, the ferromagnetic and antiferromagnetic components of the exchange interactions are rather small and of similar order of magnitude. In such a situation, small topological variations in the bridges or even the chemical nature of bridges of identical geometry could result in different prevalent interactions.[25] In fact, topological considerations in line with those in ref 5 (i.e., based mainly on the relative arrangement of the medium basal planes of the VO_6 octahedra) seems to work adequately in simple binuclear systems such as those studied by Plass.[2b] Notwithstanding, in arguing for their proposals, Papoutsakis et al.[5] suggest that previous results of our proper research on layered phosphates indicates correspondence between parallel arrangement of the basal planes of the VO_6 octahedra and ferromagnetism. This is not exact, as was clearly shown already in the case of α-$VO(HPO_4)\cdot 2H_2O$[9] or $MoOPO_4$,[10] both of which showed antiferromagnetic coupling despite the parallel arrangement of the mentioned planes. Then, the new results in this work on lamellar oxovanadium phosphates (in all cases, the coupling is antiferromagnetic) are not surprising to us. They suggest (when compared to the literature data) that the complexity of the problem is higher than the simple consideration of the relative arrangement of the VO_6 octahedra basal planes and that the topological details of the phosphate portions in the chairlike $V(OPO)_2V$ links play also a relevant role. On the other hand, there does exist a certain relation between the magnitude of the magnetic interaction (as measured by *J*, Table 1) and the mentioned dihedral angle (values of *J* are smaller for parallel arrangements). The rest of this work presents all of these considerations in quantitative terms.

Magnetostructural Correlations from Extended Hückel Calculations. According to the above, the dominant building block—in the entire set of oxovanadium(IV) phosphates we are dealing with—are the $V(OPO)_2V$ units shown in Figure 1. We have analyzed individually all the blocks labeled as D, and then each structure has been examined as resulting from the involved blocks. With this aim, we have started in each case from the crystallographic data corresponding to the entire block, i.e. to the respective VO_6 octahedra and PO_4 tetrahedra. To evaluate the effectiveness of phosphate groups as exchange pathways, our calculations include both the di-μ-$O(PO_4)$ bridges (DI, DII) and the chairlike di-μ-$(O,O')(PO_4)$ bridges (DIII−DXIII). As could be expected, the results in each one of both these series correlate independently. In the same way, our calculations corroborate the well-known inefficiency of the oxo (V═O) bridges (block O)[5,6,9,10,24] as well as that of the single phosphate bridges (M) in these series of compounds.[6,13]

Table 2. Orbital Exponents (Contraction Coefficients in Double-ζ Expansion Given in Parentheses) and Energies Used in the Extended Hückel Calculations

atom	orbital	ζ_i (c_i)	H_{ii} (eV)
O	2s	2.275	−32.30
	2p	2.275	−14.80
P	3s	1.75	−18.60
	3p	1.30	−14.00
V	4s	1.30	−8.80
	4p	1.30	−5.52
	3d	4.75(0.4560) 1.50(0.7520)	−6.70

It is well-known that in the framework of localized orthogonal magnetic orbitals a and b,[26] as proposed by Hay et al.,[27] and for symmetrical complexes, it is found that the singlet−triplet energy gap is given by the expression (1)

$$J = 2K_{ab} - \frac{\Delta^2}{J_{aa} - J_{ab}} \quad (1)$$

where Δ is the energy gap between the singly occupied molecular orbitals (SOMO's) Φ_g and Φ_u, K_{ab} is the two-electron exchange integral between a and b, and J_{aa} and J_{ab} are the two-electron Coulomb integrals defined by Hay et al.[27] The first term is always positive (ferromagnetic contribution), and the second term is negative (antiferromagnetic contribution). In series of complexes of similar geometries the two-electron integrals are assumed to be constant by Hay et al.[27] So the value of Δ^2 can be used to follow the evolution of *J* in a family of complexes. Hay et al. propose the extended Hückel methodology as a simple tool to evaluate Δ.

To analyze qualitatively the influence of structural parameters on the value of the coupling constant, we have performed extended Hückel calculations on the experimental units depicted in Figure 1 with a modified Wolfsberg−Helmholz formula to estimate the orbital interaction energies (matrix off-diagonal elements) from their energies (matrix diagonal elements, H_{ii}, and H_{jj}) and the overlapping integral between them (S_{ij}), through the equation $H_{ij} = 1.75(H_{ii} + H_{ij})S_{ij}/2$.[28] We have considered all the oxygen atoms of the bridging phosphate groups and the six oxygens describing the characteristic octahedral environment of the V atoms. The atomic parameters used are shown in Table 2. These calculations were performed using the CACAO program.[29]

(22) Kang, H. Y.; Lee, W. C.; Wang, S. L.; Lii, K. H. *Inorg. Chem.* **1992**, *31*, 4743.
(23) Wang, S. L.; Kang, H. Y.; Cheng, C. Y.; Lii, K. H. *Inorg. Chem.* **1991**, *30*, 3496.
(24) Rushbrooke, G. S.; Wood, P. J. *Mol. Phys.* **1958**, *1*, 257.
(25) Lezama, L.; Villeneuve, G.; Marcos, M. D.; Pizarro, J. L.; Hagenmuller, P. *Solid State Commun.* **1989**, *70*, 899.
(26) Girerd, J. J.; Journaux, Y.; Kahn, O. *Chem. Phys. Lett.* **1981**, 82, 534.
(27) Hay, P. J.; Thibeault, J. C.; Hoffmann, R. *J. Am. Chem. Soc.* **1975**, 97, 4884.
(28) Wolfsberg, M. H.; Helmholz, L. *J. Chem. Phys.* **1952**, 20, 837.

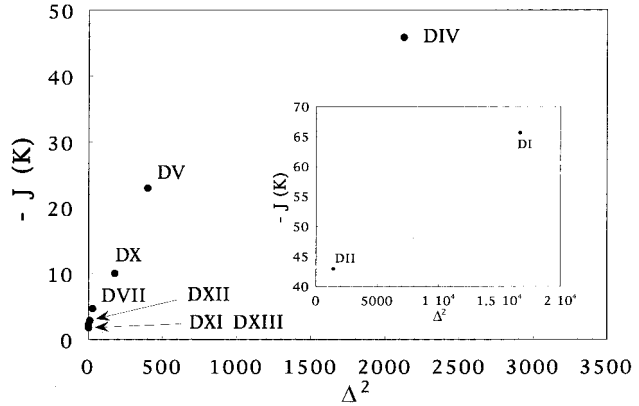

Figure 5. Plot of J(K) against Δ^2 for the magnetically active di-μ-(O,O′)PO_4 bridges (DIV($(VO)_2P_2O_7$), DV (α-$VO(HPO_4)\cdot 2H_2O$), DX ($Ba_2VO(PO_4)_2\cdot H_2O$), DVII ($VO(HPO_4)\cdot 4H_2O$), DXI ($Na(VOPO_4)_2\cdot 4H_2O$), DXII ($Ca(VOPO_4)_2\cdot 4H_2O$), and DXIII ($Ba(VOPO_4)_2\cdot 4H_2O$)). In the inset, the same plot for the active di-μ-(O)PO_4 bridges (DI ($(VO)_2P_2O_7$) and DII ($VO(HPO_4)\cdot 0.5H_2O$).

The calculated Δ^2 values for the different building blocks are used to define the abcissa in Figure 5. As can be noted, in agreement with theoretical considerations, there is a rather good correlation between the experimental J values and the Δ^2 calculated ones. In light of these Δ values, we can now revisit all those oxovanadium phosphates whose magnetic behavior is well-established, in order to explain the experimental observations.

(a) $(VO)_2P_2O_7$ and $VO(HPO_4)\cdot 0.5H_2O$ are the two compounds in these series in whose structures the di-μ-O(PO_4) bridges play an essential role. Thus, the structure of $VO(HPO_4)\cdot 0.5H_2O$[30] can be adequately described as built up from DII ($\Delta = 37.7$ meV, $J = -46.0$ K) units linked among them (in the *xy* planes) through DIII ($\Delta \approx 0$ meV) and DVIII ($\Delta \approx 0$ meV) bridges. According to these calculations, the only active path should be DII and the susceptibility data could be analyzed in terms of dimeric entities.[6] In contrast, the structure of $(VO)_2P_2O_7$ is somewhat more complex,[31] and can be thought of as being constructed from DI ($\Delta = 129.1$ meV, $J = -65.7$ K), DIV($\Delta = 46.1$ meV, $J = -46.0$ K), and DVIII ($\Delta \approx 0$ meV) building blocks. The active paths are then DI and DIV, which alternate in the structure along the (010) direction. Thus, our calculations support the phenomenological previous fit of the susceptibility data using a Heisenberg alternating $S = {}^1/_2$ chain model.[6]

(b) The cases of α-$VO(HPO_4)\cdot 2H_2O$ and $VO(HPO_4)\cdot 4H_2O$ constitute two examples of low-dimensionality magnetic systems because of the connectivity of the only di-μ-(O,O′)(PO_4) bridge type that results active in each solid. The magnetic inefficiency of both the oxo (O) and the single phosphate (M) bridges in the case of α-$VO(HPO_4)\cdot 2H_2O$ would transform a structurally bidimensional (layered) solid[32] in a magnetically dimerized system, in which the DV ($\Delta = 20.0$ meV, $J = -23.0$ K) blocks constitute the only active exchange path. In the case of $VO(HPO_4)\cdot 4H_2O$, its structure[20] involves only DVII($\Delta = 5.3$ meV, $J = -5.1$ K) repetitive units that expand along the chain direction. As in the preceding examples, these considerations are in good agreement with the experimental adjustments in the literature.[6,33]

(c) The $M(VOPO_4)_2\cdot nH_2O$ (M = Na, K, Rb, Ca, Sr, Ba) derivatives make up a set of bidimensional materials from both the structural and the magnetic points of view. All of them include chairlike di-μ-O,O′(PO_4) bridges with very similar topologies, ranging from DXII ($\Delta = 3.2$ meV, $J = -2.6$ K) to DXIII ($\Delta = 0.2$ meV, $J = -2.0$ K). In accordance with these Δ values, the resulting magnetic interactions will be very weak but, given that the respective building blocks propagate in the *xy* plane,[5,22,23] a 2-D magnetic behavior is expected, as occurs in practice.

(d) A particular case, which deserves a short comment in the light of the present considerations, is that of the barium derivative $Ba_2VO(PO_4)_2\cdot H_2O$ described by Harrison et al.[19] In contrast to the lamellar derivative $Ba(VOPO_4)_2\cdot 4H_2O$ that we are studying,[16] $Ba_2VO(PO_4)_2\cdot H_2O$ is built up from infinite chains that could be described as formed by DX ($\Delta = 13.3$ meV, $T_{(\chi_{max})} = 10$ K) interconnected building blocks. Note that the calculated Δ value is higher than those corresponding to the lamellar derivatives (DXII, DXIII) but significantly lower than that calculated for the chairlike block in the alternate chains in $(VO)_2P_2O_7$ (DIV; $\Delta = 46.1$ meV, $J = -46.0$ K, $T_{(\chi_{max})} = 70$ K). In appearance, however, DX and DIV units look very similar; in both cases the basal medium planes of adjacent VO_6 octahedra are practically coplanar and a hypothetical V to V line would bisect the OVO angles of these basal planes in both moieties. While it seems clear initially that such an arrangement can explain the relatively high coupling efficiency with regard to the available path in the lamellar derivatives (in which VO_6 octahedra stay at different level), understanding the difference in efficiency between DX and DIV requires additional arguments. What establishes the main difference between DX and DIV units is the relative orientation of the shared PO_4 groups with respect to the VO_6 octahedra. Two immediate consequences can be inferred from this observation: first, the modification of the magnitude of the magnetic interaction with the relative orientation of the PO_4 bridges must be due to changes in the effective overlap of the PO_4 group orbitals implied in the magnetic orbitals, and second, the quantitative significance of these modifications is at least of the same order as those due to relative displacements of the VO_6 octahedra. The next section contrasts these hypotheses.

Magnetic Exchange and Orbital Overlap. At this point, it seems evident that, in the real systems we are studying, the limited symmetry of the set of atoms (considered as a whole) defining the vanadium-to-vanadium connections in each case (i.e., the $V(OPO)_2V$ links) will initially allow an increased degree of mixing among many orbitals of the involved atoms. Such a complex situation advises us to break down the problem by separately analyzing different topological parameters whose variations could play a key role in determining the effective orbital overlap, and consequently on the magnitude of the superexchange magnetic interaction. The selected parameters are (a) d(Å) (Figure 6), which measures the effect of in-plane relative displacements of the medium basal planes of the VO_6 octahedra while maintaining the relative orientation of the PO_4 bridges; (b) θ (deg) (Figure 7), out-of-plane relative displacements of the VO_6 medium basal planes without changes in the PO_4 bridges; and (c) ϕ (deg) (Figure 8), which describes the tilting of the PO_4 groups with regard to fixed VO_6 octahedra.

(29) Mealli, C.; Proserpio, D. M. *Computer Aided Composition of Atomic Orbitals (CACAO Program)*, PC version; July 1992; see also *J. Chem. Educ.* **1990**, 67, 3399.
(30) Torardi, C. C.; Calabrese, J. C. *Inorg. Chem.* **1984**, *23*, 1308.
(31) (a) Gorbunova, Y. E.; Linde, S. A.; Lavrov, A. V.; Tananaev, I. V. *Dokl. Akad. Nauk SSSR* **1980**, *250*, 350. (b) Nguyen, P. T.; Hoffman, R. D.; Sleight, A. W. *Mater. Res. Bull.* **1995**, *30*, 1055.
(32) Le Bail, A.; Ferey, G.; Amorós, P.; Beltrán, D. *Eur. J. Solid State Inorg. Chem.* **1989**, *26*, 417.
(33) Wroblesky, T. *Inorg. Chem.* **1988**, *27*, 946.

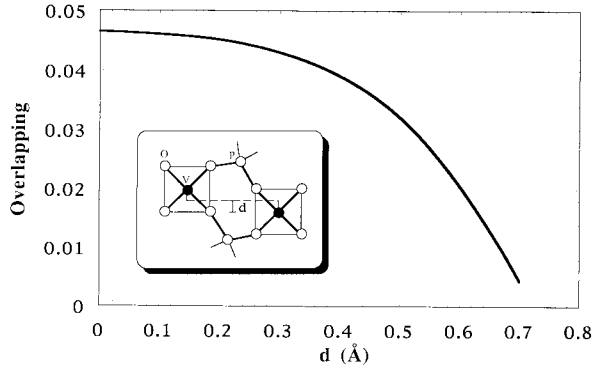

Figure 6. Plot of the overlap integral between the xy_u FMO of the vanadium atoms and the LO_u FMO of the phosphate bridging anions as a function of the relative in-plane displacement of the VO_6 octahedra (measured as *d*).

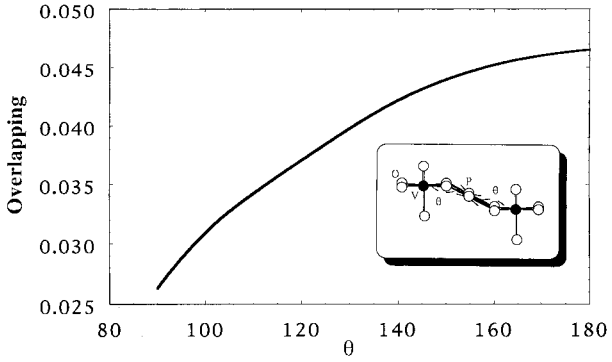

Figure 7. Plot of the overlap integral between the xy_u FMO of the vanadium atoms and the LO_u FMO of the phosphate bridging anions as a function of the relative out-of-plane displacement of the VO_6 octahedra (measured as θ).

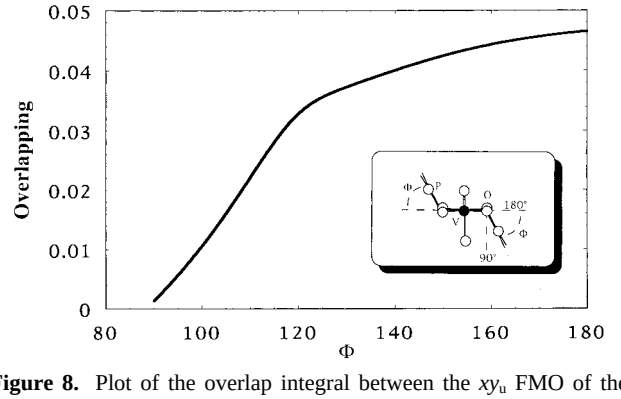

Figure 8. Plot of the overlap integral between the xy_u FMO of the vanadium atoms and the LO_u FMO of the phosphate bridging anions as a function of the relative orientation of the PO_4 groups (measured as ϕ).

It becomes clear that different values of Δ must be related to different overlap between the metal (xy_i) and the bridging ligand orbitals (LO_i) (where i = u (ungerade) or g (gerade)). We have evaluated this overlap considering that the metal FMO's (fragment orbitals) are the orbitals of the fragment formed by the two metal atoms with their peripheral ligands, except for the oxygen atoms associated to the phosphate bridging units. The xy_u FMO is basically constituted by the two d_{xy} orbitals of the vanadium atoms of the respective building block. The LO_u FMO have a high participation of the p orbitals of the oxygen atoms perpendicular to the P−O bonds. When the overlap between xy_u FMO and LO_u FMO increases, there is a major interaction between metal and bridging ligand orbitals, and, as a consequence, the value of Δ increases. On the other hand, the shift of the ^{31}P NMR signal is due to the participation of the s orbitals of the P atom in the LO_g FMO.

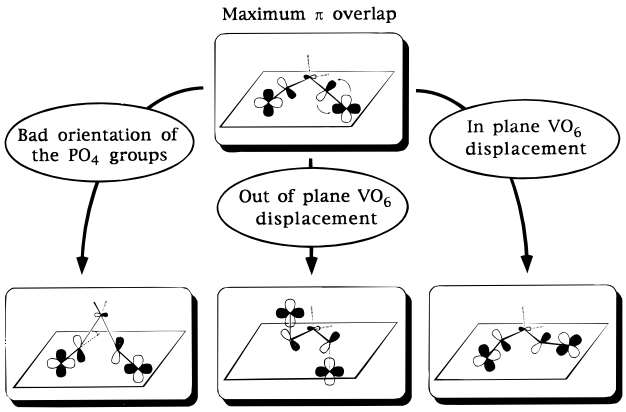

Figure 9. Schematic representation of the relative disposition of the dominant orbitals in the xy_u FMO of the vanadium atoms and the LO_u FMO of the phosphate groups in the case of the di-μ(O,O′)PO_4 bridges, showing the maximum π overlap and taking into account the three previously analyzed displacements which give rise to a decrease of the overlap integral.

As shown in Figures 6−8, these kinds of calculations reveal clear tendencies concerning the influence of topological parameters on the magnitude of the magnetic orbital overlap. Thus, the overlap is very sensitive to in-plane relative displacements of the VO_6 octahedra (Figure 6), but results were more gradual when the relative VO_6 octahedra displacements that are considered imply out-of-plane movements (Figure 7). Otherwise, a tilt of PO_4 groups produces initially a steady overlap decrease, but an abrupt decrease occurs for a ϕ value of ca. 120° (Figure 8). We have tried to schematically summarize the meaning of these considerations in Figure 9.

In light of these tendencies in the values of the overlap integrals, *S*, we can now examine more deeply some of the experimental behaviors discussed above. Thus, the 2-D magnetic behavior, which might hypothetically be expected for compounds such as $(VO)_2P_2O_7$ and $VO(HPO_4)\cdot 0.5H_2O$—di-μ-$O(PO_4)$ bridges—would be inhibited because of the poor overlap that results for DVIII blocks involving in-plane displaced VO_6 octahedra. On the other hand, *S* values are less sensitive to out-of-plane displacements of VO_6 octahedra: this would allow us to understand the progressive lowering of the *J* values along the series α-$VO(HPO_4)\cdot 2H_2O$ (DV), $VO(HPO_4)\cdot 4H_2O$ (DVII), $M(VOPO_4)_2\cdot nH_2O$ (DXII−DXIII), without affecting either the fact that all these blocks result magnetically active or that they are responsible for the resulting magnetic dimensionality. In this context, $Ba_2VO(PO_4)_2\cdot H_2O$ results in a special case. Thus, although it includes perfectly faced in-plane VO_6 octahedra, the magnitude of the magnetic interaction (*J*) is small. The main topological difference between the DIV blocks active in the $(VO)_2P_2O_7$ case ($J = -46.0$ K; $S \approx 0.046$) and those of DX type involved in $Ba_2VO(PO_4)_2\cdot H_2O$ ($J \approx -(8-10)$ K; $S \approx 0.020$) lies in the relative orientation of the phosphate bridges. While the resulting situation in $(VO)_2P_2O_7$ is close to that leading to maximum π overlap between the xy_u FMO and LO_u FMO, as indicated in Figures 8 and 9, it is the poor overlap induced by the relative tilt of the PO_4 bridges in $Ba_2VO(PO_4)_2\cdot H_2O$ that results in the significant decrease of the magnitude of the magnetic interaction.

On the other hand, it is evident that, when the real building blocks (i.e., DVII, DVIII and DXII in Figure 1) are constructed in such a way that they involve simultaneously two or more undesired effects (i.e., relative in-plane or out-of-plane displace-

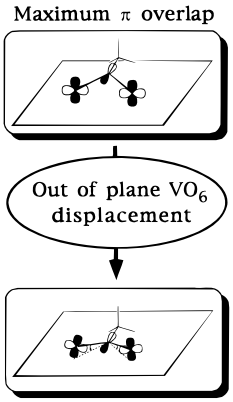

Figure 10. Schematic representation of the metal and phosphate fragments in the case of the di-μ(O)PO_4 bridges. The maximum π overlap case is observed in practice for DI ($(VO)_2P_2O_7$) and the out-of-plane VO_6 displacement leads to a situation close to that observed in the DII building block ($VO(HPO_4)\cdot 0.5H_2O$).

ments of the VO_6 octahedra or tilting of the PO_4 bridging groups), there will occur a cooperative pronounced decrease of both *S* and Δ values, which in turn may explain the low *J* values (<5 K) estimated from the χ vs *T* experimental data.

Besides the di-μ-(O, O′)PO_4 bridges, those of the type di-μ-(O)PO_4 (that is to say, those implying mainly only one of the oxygen atoms of each phosphate group in the vanadium to vanadium connection, $V(O_{PO_4})_2V$) are also relevant in the present context (DI and DII, Figure 1), although they are less common than the first ones in the families of solids we are dealing with (DI in $(VO)_2P_2O_7$ and DII in $VO(HPO_4)\cdot 0.5H_2O$). From the many available data concerning coordination compounds,[2,4] it seems reasonable to think that the bridges of the type di-μ-(O)-PO_4 can constitute exchange pathways more effective than those established through di-μ-(O,O′)PO_4 bridges, which imply a greater number of atoms in a longer path.

In practice, by applying the same kind of considerations as above, the calculated Δ values for DI (129.1 meV) and DII (37.7 meV) are significantly higher than those found for the building blocks involving di-μ-(O,O′)PO_4 bridges (ranging from ≥ 0 to ≈ 50 K, see above). To evaluate the overlap, we have considered now the d_{xy} orbitals of the vanadium atoms (xy_u FMO) and all the bridging ligand orbitals (LO_u FMO) (although only one oxygen atom per phosphate group seems to be implied in the bridging, we have considered in each case, DI and DII, all the atoms of the two PO_4 groups to perform our calculations). As expected, the LO_u FMO have a majority contribution from the p orbitals of the oxygen bridging atoms that lie along the P−O bonds. They are basically these orbitals that match up with the xy_u FMO to give the π^* overlap, this defining an effective exchange pathway (see Figure 10). The fact that the basal medium planes of the VO_6 octahedra are practically coplanar in DI ($(VO)_2P_2O_7$) represents a situation more favorable than that of DII (dihedral angle ca. 60°, $VO(HPO_4)\cdot 0.5H_2O$). This results in the calculated *S* and Δ values, significantly lower for $VO(HPO_4)\cdot 0.5H_2O$ than in the case of $(VO)_2P_2O_7$, which is in good agreement with the observed variation (Figure 5) in the respective *J* values.

Concluding Remarks

The usefulness of magnetostructural correlations such as those discussed in this work may be tested by considering additional examples of vanadium phosphates that fit in well with our main working hypothesis, that is to say vanadium phosphates in whose structures only be involved PO_4 groups as bridging entities between metallic atoms (apart from oxygen atoms of the V=O fragments). Thus, β-$LiVOPO_4$ is a 3D solid whose structure can be thought of as constructed from VO_6 octahedra connected among them through di-μ-(O,O′)PO_4 bridges defining linear chains.[34] The medium basal planes of the VO_6 octahedra in these chains are not in-plane displaced ($d = 0$ A, Figure 6), but they are placed at a different level ($\theta = 130°$, Figure 7) and the relative orientation of the PO_4 bridging groups is intermediate ($\theta = 127°$) between those of DIV in $(VO)_2P_2O_7$ and DX in $Ba_2VO(PO_4)_2\cdot H_2O$. With regard to the ideal situation ($\theta = 180°$ and $\phi = 180°$, maximum overlap ($S = 0.046$), Figures 7 and 8), these effects would imply *S* cooperative reductions of approximately 24% and 18%, which allow us to estimate a *J* value close to −29 K. This value is very similar to that experimentally found by adjusting the magnetic susceptibility data with a 1-D model ($J_{exp} = -31.9$ K).[34]

In a similar way, it is possible to apply these ideas in order to make approximate predictions about the magnitude of the magnetic interactions, starting from structural data, in cases for which experimental *J* values are unknown. For example, the structure of $Ba_8(VO)_6(PO_4)_2(HPO_4)_{11}\cdot 3H_2O$ involves two topologically very similar types of VO_6 chains defined through di-μ-(O,O′)PO_4 bridges.[35] The VO_6 octahedra in these chains present an optimum relative disposition in that concerning to the possible magnetic interactions: they are well faced, and their medium basal planes stay at the same level. However, the PO_4 bridging groups appear tilted ($\phi = 115°$), if their relative orientation is somewhat more favorable than that observed in the case of $Ba_2VO(PO_4)_2\cdot H_2O$ ($\phi = 108°$). Taking into account the experimental ϕ medium value, it is possible to estimate an *S* decrease close to 44% of the expected value in the ideal arrangement ($\phi = 180°$; $S = 0.046$). This would result in an expected *J* value in the −15 to −20 K range, which seems to be a reasonable prediction in the light of the observed $T_{\chi_{max}}$ product near 20 K.

Acknowledgment. This work was supported by grants GV-2227/94 and PB95-1094 from the Generalitat Valènciana and the DGICYT, respectively. M.D.M. thanks the Spanish Ministerio de Educación y Ciencia for a postdoctoral contract.

IC971210O

(34) Lii, K. H.; Li, C. H.; Cheng, C. Y.; Wang, S. L. *J. Solid State Chem.* **1991**, *95*, 352.
(35) Harrison, W. T. A.; Vaughey, J. T.; Jacobson, A. J.; Goshorn, D. P.; Johnson, J. W. *J. Solid State Chem.* **1995**, *116*, 77.